Journal of Solid Mechanics Vol. 5, No. 3 (2013) pp. 226-244

Wave Propagation at an Interface of Elastic and Microstretch Thermoelastic Solids with Microtemperatures

R. Kumar[1], M. Kaur[2,*], S.C. Rajvanshi[3]

[1]*Department of Mathematics, Kurukshetra University, Kurukshetra 136119, India*
[2]*Department of Applied Sciences, Guru Nanak Dev Engineering College, Ludhiana, Punjab 141008, India*
[3]*Department of Applied Sciences, Gurukul Vidyapeeth Institute of Engineering and Technology, Sector-7, Banur, District Patiala, Punjab 140601, India*

Received 7 May 2013; accepted 1 July 2013

ABSTRACT

In the present paper, the problem of reflection and transmission of waves at an interface of elastic and microstretch thermoelastic solids with microtemperatures has been studied. The amplitude ratios of various reflected and transmitted waves are functions of angle of incidence and frequency of incident wave. The expressions of amplitude ratios have been computed numerically for a particular model. The variations of amplitude ratios with angle of incidence are shown graphically to depict the effect of microrotation. Some particular cases of interest have been also deduced.

Keywords: Microstretch; Microtemperatures;Wave propagation; Amplitude ratios; Elastic solid

1 INTRODUCTION

ERINGEN [1, 2] developed the theory of micromorphic bodies. The theory of microstretch elastic bodies developed by Eringen [3] is a generalization of the micropolar theory. Eringen [4] also developed the theory of thermomicrostretch elastic solids. The particles of microstretch materials have seven degree of freedom: three displacements, three microrotations and one microstretch. A microstretch continuum can model composite materials reinforced with chopped elastic fibres and various porous solids. The material points of these bodies can stretch and contract independently of their translations and rotations.

Grot [5] established a theory of thermodynamics of elastic bodies with microstructure whose microelements possess microtemperatures. The Clausius–Duhem inequality is modified to include microtemperatures and the first-order moment of the energy equations are added to the usual balance laws of a continuum with microstructure.

Riha [6] presented a study of heat conduction in materials with microtemperatures. Experimental data for the silicone rubber containing spherical aluminium particles and for human blood were found to conform closely to predicted theoretical thermal conductivity.The linear theory of thermoelasticity with microtemperatures for materials with inner structure whose particles possess microtemperatures, in addition to the classical displacement and temperature fields, was constructed by Iesan and Quintanilla [7]. Various investigators have studied different types of problems in microstretch thermoelastic medium notable among them are Ciarletta and Scalia [8], Iesan and Quintanilla [9], Othman et al [10], Passarella and Tibullo [11], Marin [12,13], Kumar et al [14], Othman and Lofty [15,16], Kumar and Rupender [17,18], Shaw and Mukhopadhayay [19].

Iesan [20] discussed the theory of micromorphic elastic solids with microtemperatures, Iesan and Quintanilla [21] discussed various problems using thermoelasticity with microtemperatures. Exponential stability in thermoelasticity with microtemperatures was studied by Casas and Quintanilla [22]. Scalia and Svandze [23]

* Corresponding author. Tel.: +91 9463055900.
E-mail address: mandeep1125@yahoo.com (M. Kaur).

presented the solutions of the theory of thermoelasticity with microtemperatures, Iesan [24] discussed thermoelasticity of bodies with microstructure and microtemperatures. Aouadi [25] studied some theorems in the isotropic theory of microstretch thermoelasticity with microtemperatures. Scalia et al [26] discussed basic theorems in the equilibrium theory of thermoelasticity with microtemperatures. The growth and continous dependence in thermoelasticity with microtemperatures was discussed by Quintanilla [27]. Steeb et al [28] studied time harmonic waves in thermoelastic material with microtemperatures. Chirita et al [29] studied the theory of thermoelasticity with microtemperatures.

The main objective of the present investigation is to study the wave propagation at the boundary between a microstretch thermoelastic half-space with microtemperatures and elastic solid half-space. The amplitude ratios of longitudinal displacement wave (LD-wave), thermal wave (T-wave), microstretch wave (LM-wave), microtemperature wave (LT-wave), coupled transverse displacement, microrotational wave and microtemperature wave namely (CD-I wave, CD-II wave and CD-III wave) and transmitted longitudinal wave (P-wave) and transverse wave (SV-wave) have been obtained and plotted graphically with angle of incidence. Some special cases of interest have been deduced from the present investigation.

2 BASIC EQUATIONS

Following Eringen [5] and Iesan [30], the field equations and constitutive relations for a homogeneous, isotropic microstretch thermoelastic solid with microtemperatures without body forces, body couples, stretch force, heat sources and first heat source moment, can be written as:

$$(\lambda+2\mu+K)\nabla(\nabla \boldsymbol{u})-(\mu+K)\nabla\times(\nabla\times\boldsymbol{u})+K(\nabla\times\boldsymbol{\varphi})+\lambda_0\nabla\phi^*-\nu\nabla T=\rho\frac{\partial^2\boldsymbol{u}}{\partial t^2}, \tag{1}$$

$$(\alpha+\beta+\gamma)\nabla(\nabla.\boldsymbol{\varphi})-\gamma\nabla\times(\nabla\times\boldsymbol{\varphi})+K(\nabla\times\boldsymbol{u})-2K\boldsymbol{\varphi}-\mu_1(\nabla\times\boldsymbol{w})=\rho j\frac{\partial^2\boldsymbol{\varphi}}{\partial t^2}, \tag{2}$$

$$\alpha_0\nabla^2\phi^*+\nu_1 T-\lambda_1\phi^*-\lambda_0(\nabla\boldsymbol{u})-\mu_2(\nabla\boldsymbol{w})=\rho\frac{j_0}{2}\frac{\partial^2\phi^*}{\partial t^2}, \tag{3}$$

$$K^*\nabla^2 T-\rho c^*\frac{\partial T}{\partial t}-\nu_1 T_0\frac{\partial\phi^*}{\partial t}-\nu T_0(\nabla\boldsymbol{u})+k_1(\nabla\boldsymbol{w})=0, \tag{4}$$

$$k_6\nabla^2\boldsymbol{w}+(k_4+k_5)\nabla(\nabla\boldsymbol{w})+\mu_1\frac{\partial}{\partial t}(\nabla\times\boldsymbol{\varphi})-\mu_2\frac{\partial}{\partial t}(\nabla\phi^*)-b\frac{\partial\boldsymbol{w}}{\partial t}-k_2\boldsymbol{w}-k_3\nabla T=0, \tag{5}$$

and the constitutive relations are

$$t_{ij}=\lambda u_{r,r}\delta_{ij}+\mu(u_{i,j}+u_{j,i})+K(u_{j,i}-\varepsilon_{ijr}\phi_r)-\nu T\delta_{ij}+\lambda_0\phi^*\delta_{ij}, \tag{6}$$

$$m_{ij}=\alpha\phi_{r,r}\delta_{ij}+\beta\phi_{i,j}+\gamma\phi_{j,i}+b_0\varepsilon_{mji}\phi^*_{,m}, \tag{7}$$

$$\lambda^*_i=\alpha_0\phi^*_{,i}+b_0\varepsilon_{ijm}\phi_{j,m}, \tag{8}$$

$$q_{ij}=-k_4 w_{r,r}\delta_{ij}-k_5 w_{i,j}-k_6 w_{j,i}, \qquad i,j,m=1,2,3 \tag{9}$$

where $K,\alpha,\beta,\gamma,\lambda,\mu,\alpha_0,\lambda_0,\lambda_1,\mu_1,\mu_2,j_0,k_i\,(i=1,..........,6)$ are constitutive coefficients. t_{ij} and m_{ij} are the components of stress tensor and couple stress tensor, λ^*_i is the microstress tensor, q_{ij} is the first heat flux moment tensor, $\boldsymbol{u}$ and $\boldsymbol{\varphi}$ are the displacement and microrotation vectors, $\boldsymbol{w}$ is the microtemperature vector and ϕ^* is the microstretch scalar, ρ is the density, j is the microinertia, c^* is the specific heat at constant strain, K^* is the thermal conductivity, T is the thermodynamic temperature, T_0 is the reference temperature, $\nu=(3\lambda+2\mu+K)\alpha_{T_1}$, $\nu_1=(3\lambda+2\mu+K)\alpha_{T_2}$, where α_{T_1}, α_{T_2} are the coefficients of linear thermal expansion.

Following Bullen [31], the equation of motion and constitutive relation in an isotropic elastic solid are given by:

$$(\lambda^e+\mu^e)\nabla\left(\nabla \boldsymbol{u}^{\boldsymbol{e}}\right)+\mu^e\nabla^2\boldsymbol{u}^{\boldsymbol{e}}=\rho^e\frac{\partial^2\boldsymbol{u}^{\boldsymbol{e}}}{\partial t^2}, \tag{10}$$

$$t_{ij}^{\ e}=\lambda^e u_{r,r}^e\delta_{ij}+\mu^e\left(u_{i,j}^e+u_{j,i}^e\right), \tag{11}$$

where λ^e, μ^e are Lame's constants, $\boldsymbol{u}^{\boldsymbol{e}}$ is the displacement vector, ρ^e is density corresponding to isotropic elastic solid.

3 FORMULATION OF THE PROBLEM AND SOLUTION

We consider an isotropic elastic solid half-space lying over a homogeneous isotropic, microstretch thermoelastic half-space with microtemperatures. The origin of the Cartesian coordinate system $Ox_1x_2x_3$ is taken at any point on the plane surface (interface) and x_3-axis points vertically downwards into the microstretch thermoelastic half-space with microtemperatures is introduced. The region $x_3\geq 0$ is occupied by microstretch thermoelastic half-space with microtemperatures (medium M_1) and an elastic solid half-space occupies the region $x_3\leq 0$ (medium M_2) as shown in Fig. 1. We consider plane waves in the x_1x_3-plane with wave front parallel to the x_2-axis.

For two dimensional problem, we take

$$\boldsymbol{u}=\left(u_1(x_1,x_3),0,u_3(x_1,x_3)\right),\quad \boldsymbol{w}=\left(w_1(x_1,x_3),0,w_3(x_1,x_3)\right),\qquad \boldsymbol{\varphi}=\left(0,\phi_2(x_1,x_3),0\right)$$
$$\boldsymbol{u}^{\boldsymbol{e}}=\left(u_1^e(x_1,x_3),0,u_3^e(x_1,x_3)\right) \tag{12}$$

We define the dimensionless quantities as:

$$x_1'=\frac{x_1}{L},\quad x_3'=\frac{x_3}{L},\quad (u_1',u_3')=(u_1,u_3)\frac{1}{L},\quad (u_1^{e'},u_3^{e'})=(u_1^e,u_3^e)\frac{1}{L},\quad \phi_2'=\phi_2,$$
$$\phi^{*'}=\phi^*,\quad t_{ij}'=\frac{1}{\nu T_0}t_{ij},\quad m_{ij}'=\frac{1}{L\nu T_0}m_{ij},\quad \lambda_i^{*'}=\frac{1}{L\nu T_0}\lambda_i,\quad q_{ij}'=\frac{1}{Lc_1\nu T_0}q_{ij}, \tag{13}$$
$$t_{ij}^{e'}=\frac{1}{\nu T_0}t_{ij}^e,\quad t'=\frac{c_1}{L}t,\quad T'=\frac{T}{T_0},\quad w_i'=Lw_i,\quad L=\left(\frac{b}{\rho c^*T_0}\right)^{\frac{1}{2}},\quad c_1^2=\frac{\lambda+2\mu+K}{\rho}$$

The relations connecting displacement components and microtemperature components to the potential functions in dimensionless form are expressed as:

$$u_1=\frac{\partial\phi}{\partial x_1}-\frac{\partial\psi}{\partial x_3},\quad u_3=\frac{\partial\phi}{\partial x_3}+\frac{\partial\psi}{\partial x_1},\quad w_1=\frac{\partial\phi_1}{\partial x_1}-\frac{\partial\psi_1}{\partial x_3},\quad w_3=\frac{\partial\phi_1}{\partial x_3}+\frac{\partial\psi_1}{\partial x_1},\quad u_1^e=\frac{\partial\phi^e}{\partial x_1}-\frac{\partial\psi^e}{\partial x_3},\quad u_3=\frac{\partial\phi^e}{\partial x_3}+\frac{\partial\psi^e}{\partial x_1} \tag{14}$$

where the primes have been suppressed. Using the dimensionless quantities given by Eq. (13) in Eqs. (1)-(5),(10),(11) and with the aid of Eq. (12) and (14), we obtain the following equations

$$[(a_1+1)\nabla^2-a_5\frac{\partial^2}{\partial t^2}]\phi+a_3\phi^*-a_4T=0, \tag{15}$$

$$(\nabla^2-a_5\frac{\partial^2}{\partial t^2})\psi+a_2\phi_2=0, \tag{16}$$

$$(\nabla^2 - 2a_6 - a_8 \frac{\partial^2}{\partial t^2})\phi_2 - a_6\nabla^2\psi + a_7\nabla^2\psi_1 = 0, \tag{17}$$

$$(\nabla^2 - a_{10} - a_{13} \frac{\partial^2}{\partial t^2})\phi^* - a_{11}\nabla^2\phi - a_{12}\nabla^2\phi_1 + a_9 T = 0, \tag{18}$$

$$(\nabla^2 - a_{14} \frac{\partial}{\partial t})T - a_{15} \frac{\partial \phi^*}{\partial t} - a_{16}\nabla^2\phi + a_{17}\nabla^2\phi_1 = 0, \tag{19}$$

$$[\nabla^2(1 + a_{18}) - a_{21} - a_{23} \frac{\partial}{\partial t}]\phi_1 - a_{20} \frac{\partial \phi^*}{\partial t} - a_{22} T = 0, \tag{20}$$

$$(\nabla^2 - a_{21} - a_{23} \frac{\partial}{\partial t})\psi_1 + a_{19} \frac{\partial \phi_2}{\partial t} = 0, \tag{21}$$

$$(\nabla^2 - \frac{\partial^2}{\partial t^2})\phi^e = 0, \tag{22}$$

$$(\nabla^2 - \bar{a}_1 \frac{\partial^2}{\partial t^2})\psi^e = 0, \tag{23}$$

where

$$a_1 = \frac{\lambda + \mu}{\mu + K}, \quad a_2 = \frac{K}{\mu + K}, \quad a_3 = \frac{\lambda_0}{\mu + K}, \quad a_4 = \frac{\nu T_0}{\mu + K}, \quad a_5 = \frac{\rho c_1^2}{\mu + K}, \quad a_6 = \frac{KL^2}{\gamma},$$

$$a_7 = \frac{\mu_1}{\gamma}, \quad a_8 = \frac{\rho j c_1^2}{\gamma}, \quad a_9 = \frac{\nu_1 T_0 L^2}{\alpha_0}, \quad a_{10} = \frac{\lambda_1 L^2}{\alpha_0}, a_{11} = \frac{\lambda_0 L^2}{\alpha_0}, \quad a_{12} = \frac{\mu_2}{\alpha_0}, \quad a_{13} = \frac{\rho j_0 c_1^2}{2\alpha_0},$$

$$a_{14} = \frac{\rho c^* c_1 L}{K^*}, \quad a_{15} = \frac{\nu_1 c_1 L}{K^*}, \quad a_{16} = \frac{\nu c_1 L}{K^*}, \quad a_{17} = \frac{k_1}{K^* T_0}, \quad a_{18} = \frac{k_4 + k_5}{k_6}, \quad a_{19} = \frac{\mu_1 c_1 L}{k_6},$$

$$a_{20} = \frac{\mu_2 c_1 L}{k_6}, \quad a_{21} = \frac{k_2 L^2}{k_6}, \quad a_{22} = \frac{k_3 T_0 L^2}{k_6}, \quad a_{23} = \frac{b c_1 L}{k_6}, \quad \bar{a}_1 = \frac{\lambda^e + \mu^e}{\mu^e}, \quad \bar{a}_1 = \frac{\rho^e c_1^2}{\mu^e}$$

The boundary conditions at the interface $x_3 = 0$ are given as:

$$t_{33} = t_{33}^e, \quad t_{31} = t_{31}^e, \; m_{32} = 0, \; \lambda_3^* = 0, \quad q_{33} = 0, \quad q_{31} = 0, \quad u_3 = u_3^e, \quad u_1 = u_1^e,$$
$$\frac{\partial T}{\partial x_3} = 0 \tag{24}$$

4 REFLECTION AND TRANSMISSION

We consider longitudinal displacement wave (LD-wave), thermal wave (T-wave), microstretch wave (LM-wave), microtemperature wave (LT-wave), coupled transverse displacement, microrotational wave and microtemperature wave namely (CD-I wave, CD-II wave and CD-III wave) propagating through medium M_1 and incident at the plane $x_3 = 0$ with its direction of propagation with angle θ_0 normal to the surface. Corresponding to each incident wave, we get reflected LD-wave, T-wave, LM-wave, LT-wave, CD-I, CD-II and CD-III waves in medium M_1 and transmitted P- wave and SV-wave in medium M_2 as shown in Fig. 1.

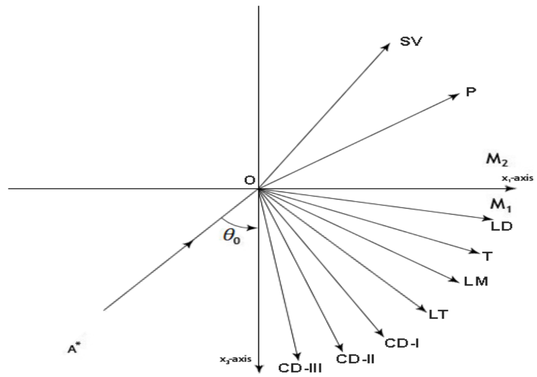

Fig. 1
Geometry of the problem.

In order to solve the Eqs. (15)-(23), we assume the solutions of the form

$$\{\phi, T, \phi^*, \phi_1, \psi, \phi_2, \psi_1, \phi^e, \psi^e\} = \{\bar{\phi}, \bar{T}, \overline{\phi^*}, \overline{\phi_1}, \bar{\psi}, \overline{\phi_2}, \overline{\psi_1}, \overline{\phi^e}, \overline{\psi^e}\} e^{\iota\{k(x_1 \sin\theta - x_3 \cos\theta) - \omega t\}} \tag{25}$$

where k is the wave number and ω is the angular frequency and $\bar{\phi}, \bar{T}, \overline{\phi^*}, \overline{\phi_1}, \bar{\psi}, \overline{\phi_2}, \overline{\psi_1}, \overline{\phi^e}, \overline{\psi^e}$ are arbitrary constants.

Making use of Eq. (25) in Eqs (15)-(23), yield

$$B_1V^8 + B_2V^6 + B_3V^4 + B_4V^2 + B_5 = 0\,, \tag{26}$$

$$D_1V^6 + D_2V^4 + D_3V^2 + D_4 = 0\,, \tag{27}$$

where

$$B_1 = \iota a_{21}^* \frac{a_5}{\omega^5}(a_{13}^* a_{14}^* - a_9),\ B_2 = -\frac{a_5}{\omega^2} a_{13}^* \delta_3 + \iota \frac{a_5}{\omega^3}\delta_4 + \frac{a_{12}}{\omega^2}\delta_5 - \frac{a_3}{\omega^5} a_{21}^* \delta_6 + \frac{a_4}{\omega^4} a_{21}^* (a_{13}^* a_{16} - a_{11} a_{15} \frac{\iota}{\omega}),$$

$$B_3 = -\frac{a_1^*}{\omega^2} a_{13}^* \delta_3 - \iota \frac{a_1^*}{\omega^3}\delta_4 - \frac{a_1^* a_{12}}{\omega^2}\delta_5 + a_5(\delta_3 + \delta_7) + \frac{a_3 a_{16}}{\omega^4}(a_{12} a_{22} - a_9 a_{18}^*) + \frac{a_3 a_{11}}{\omega^2}\delta_3 - a_4 \delta_8,$$

$$B_4 = \frac{a_{18}^*}{\omega^2}(a_4 a_{16} - a_3 a_{11}) - a_5 a_{18}^* - \frac{\iota a_1^*}{\omega}(a_{12} a_{20} + a_{14} a_{18}^*) - \frac{a_1^* \delta_1}{\omega^2} - \frac{a_1^* a_{13}^* a_{18}^*}{\omega^2},\quad B_5 = a_1 a_{18}^*,$$

$$a_1^* = a_1 + 1,\ a_{13}^* = a_{13}\omega^2 - a_{10},\ a_{14}^* = a_{14}\iota\omega,\ a_{15}^* = a_{15}\iota\omega,\ a_{18}^* = a_{18} + 1,\ a_{20}^* = a_{20}\iota\omega,\ a_{21}^* = a_{23}\iota\omega^2 - a_{21},$$

$$\delta_1 = -a_{22} a_{17} + a_{21}^*,\quad \delta_2 = a_{15} a_{18}^* + a_{17} a_{20},\ \delta_3 = (a_{14} a_{18}^* \frac{\iota}{\omega} + \frac{\delta_1}{\omega^2}),\ \ \delta_4 = (a_9 \delta_2 - a_{14} a_{21}^*),\ \ \delta_5 = (a_{14} a_{20} - a_{15} a_{22} \frac{1}{\omega}),$$

$$\delta_6 = (a_{11} a_{14} \iota - a_9 a_{16}),\quad \delta_7 = (a_{13} a_{18}^* \frac{1}{\omega^2} + a_{12} a_{20} \frac{\iota}{\omega}),\qquad \delta_8 = (a_{13}^* a_{18}^* + a_{21}^*)\frac{a_{16}}{\omega^4} + (a_{12} a_{16} a_{20} - a_{11}\delta_2)\frac{\iota}{\omega^3},$$

$$D_1 = a_5(\frac{2a_6}{\omega^2} - a_8)(\frac{a_{21}}{\omega^2} + \frac{\iota a_{23}}{\omega}),\ D_2 = -(\frac{2a_6}{\omega^2} - a_8)(\frac{a_{21}}{\omega^2} - \frac{\iota a_{23}}{\omega}) + \iota a_5(\frac{-a_{23} - a_7 a_{19}}{\omega}) - a_5 a_8 + \frac{a_2 a_6}{\omega^3}(-\iota a_{23} + \frac{a_{21}}{\omega}) + a_5(\frac{a_{21} + 2a_6}{\omega^2}),$$

$$D_3 = \frac{a_2 a_6}{\omega^2} - (\frac{a_{21}}{\omega^2} - \frac{\iota a_{23}}{\omega}) - (\frac{2a_6 - \iota a_7 a_{19}\omega}{\omega^2}) + a_5 + a_8,\qquad D_4 = -1$$

and

$$V^2 = \frac{\omega^2}{k^2}$$

Eq. (26) is biquadratic in V^2, therefore the roots of this equation gives four values of V^2. Corresponding to each value of V^2, there exist four types of waves in medium M_1 in decreasing order of their velocities, namely LD-wave, T-wave, LM-wave, LT-wave. Eq. (27) is cubic in V^2, corresponding to each value of V^2, there exist three types of waves in medium M_1 , namely CD-I wave, CD-II wave and CD-III wave. Let V_1 , V_2, V_3 , V_4 are the velocities of reflected LD-wave, T-wave, LM-wave, LT-wave and V_5, V_6, V_7 are the velocities of reflected CD-I wave, CD-II wave, CD-III wave in medium M_1. Similarly, $\overline{V_1} = 1$ is the velocity of transmitted P-wave and $\overline{V_2} = \frac{1}{a_2}$ is the velocity of SV-wave in medium M_2.

In view of Eq. (25), the appropriate solutions of Eqs. (15)-(23) for medium M_1 and medium M_2 take the form

Medium M_1:

$$\{\phi, T, \phi^*, \phi_1\} = \sum_{i=1}^{4} \{1, l_i, g_i, f_i\} [S_{0i} e^{\iota\{k_i(x_1 \sin\theta_{0i} - x_3 \cos\theta_{0i}) - \omega_i t\}} + P_i], \tag{28}$$

$$\{\psi, \phi_2, \psi_1\} = \sum_{j=5}^{7} \{1, n_j, m_j\} [S_{0j} e^{\iota\{k_j(x_1 \sin\theta_{0j} - x_3 \cos\theta_{0j}) - \omega_j t\}} + P_j], \tag{29}$$

where

$$g_i = \frac{[a_1 - a_5 V_i^2 - a_4(a_{11}a_{17} + a_{12}a_{16})][-a_{12} + \iota a_{14}a_{12}\frac{V_i^2}{\omega_i} + a_9 a_{17}\frac{V_i^2}{\omega_i^2}]}{a_3 a_{12}\frac{V_i^2}{\omega_i^2}(\iota\frac{V_i^2}{\omega_i^2} - 1) + a_{17}\frac{V_i^2}{\omega_i^2}[(a_3 a_9 - a_4 a_{10})\frac{V_i^2}{\omega_i^2} - a_4] + \iota a_4 a_{12} a_{15}\frac{V_i^4}{\omega_i^3} + a_4 a_{13} a_{17}\frac{V_i^4}{\omega_i^2}},$$

$$f_i = \frac{a_{11}a_{22}[\eta_1\eta_2 - \iota a_9 a_{15}\frac{V_i^4}{\omega_i^3}] + [-a_9 a_{16}\frac{V_i^2}{\omega_i^2} - a_{11}\eta_2][a_{22}\eta_1 + \iota a_9 a_{20}\frac{V_i^2}{\omega_i})]}{[a_9\eta_3 + a_{21}a_{22}][\eta_1\eta_2 - \iota a_9 a_{15}\frac{V_i^4}{\omega_i^3}] - [a_{12}\eta_2 + a_9 a_{17}\frac{V_i^2}{\omega_i^2}][a_{22}\eta_1 + \iota a_9 a_{20}\frac{V_i^2}{\omega_i}]},$$

$$\eta_1 = (-1 - a_{10}\frac{V_i^2}{\omega_i^2} + a_{13}V_i^2), \quad \eta_2 = (-1 + \iota a_{14}\frac{V_i^2}{\omega_i}), \quad \eta_3 = (-a_{18}^* - a_{21}\frac{V_i^2}{\omega_i^2} + \iota a_{23}\frac{V_i^2}{\omega_i}),$$

$$l_i = \frac{-\iota\omega_i(a_5 V_i^2 - a_1^*)[(-a_{17}a_{20} + a_{15}a_{21})\frac{V_i^2}{\omega_i^2} - a_{15}\eta_3] - a_3 a_6\eta_3}{-(-a_{17}a_{20} + a_{15}a_{21}\frac{V_i^2}{\omega_i^2})a_4\frac{V_i^2}{\omega_i} - \iota a_4 a_{15}\eta_3\frac{V_i^2}{\omega_i} + a_3\eta_3(-1 + \iota a_{14}\frac{V_i^2}{\omega_i}) - a_3 a_{17}a_{22}\frac{V_i^2}{\omega_i^2}},$$

$$m_j = \frac{-a_2 a_6\frac{V_j^2}{\omega_j^2} + (-1 + a_5 V_j^2)(-1 - 2a_6\frac{V_j^2}{\omega_j^2} + a_8 V_j^2) + a_7 a_{19}\iota\frac{V_j^2}{\omega_j}}{a_2 a_7\frac{V_j^2}{\omega_j^2}(a_{21}\frac{V_j^2}{\omega_j^2} - \iota a_{23}\frac{V_j^2}{\omega_j})}, \quad n_j = \frac{a_6(1 + a_{21}\frac{V_j^2}{\omega_j^2} - \iota a_{23}\frac{V_j^2}{\omega_j}) + \iota a_7 a_{19}\frac{\omega_j}{a_2}(-1 + a_5 V_j^2)}{(1 + 2a_6\frac{V_j^2}{\omega_j^2} - a_8 V_j^2)(1 + a_{21}\frac{V_j^2}{\omega_j^2} - \iota a_{23}\frac{V_j^2}{\omega_j})},$$

and

$$P_i = S_i e^{\iota\{k_i(x_1 \sin\theta_i + x_3 \cos\theta_i) - \omega_i t\}}, \qquad P_j = S_j e^{\iota\{k_j(x_1 \sin\theta_j + x_3 \cos\theta_j) - \omega_j t\}}$$

Medium M_2 :

$$\bar{\phi} = \bar{S}_1 e^{\iota\{\bar{k}_1(x_1 \sin\bar{\theta}_1 - x_3 \cos\bar{\theta}_1) - \bar{\omega}_1 t\}}, \tag{30}$$

$$\bar{\psi} = \bar{R}_1 e^{\iota\{\bar{k}_2(x_1 \sin\bar{\theta}_2 - x_3 \cos\bar{\theta}_2) - \bar{\omega}_2 t\}}, \tag{31}$$

where S_{0i} , S_{0j} are the amplitudes of incident (LD-wave, T-wave, LM-wave, LT-wave) and (CD-I, CD-II, CD-III) waves respectively. S_i and S_j are the amplitudes of reflected (LD-wave, T-wave, LM-wave, LT-wave) and (CD-I, CD-II, CD-III) waves and $\bar{S}_1$, $\bar{R}_1$ are the amplitudes of transmitted P-wave and SV-wave respectively.

We use the following extension of the Snell's law

$$\frac{\sin\theta_0}{V_0} = \frac{\sin\theta_1}{V_1} = \frac{\sin\theta_2}{V_2} = \frac{\sin\theta_3}{V_3} = \frac{\sin\theta_4}{V_4} = \frac{\sin\theta_5}{V_5} = \frac{\sin\theta_6}{V_6} = \frac{\sin\theta_7}{V_7} = \frac{\sin\bar{\theta}_1}{\bar{V}_1} = \frac{\sin\bar{\theta}_2}{\bar{V}_2} \tag{32}$$

where

$$V_j = \frac{\omega}{k_j}, \bar{V}_1 = \frac{\omega}{\bar{k}_1}, \bar{V}_2 = \frac{\omega}{\bar{k}_2} \qquad (j = 1,\ 2,\ 3,\ 4,\ 5,\ 6,\ 7) \text{ at } x_3 = 0 \tag{33}$$

Making use of Eqs. (28)-(31) in boundary conditions (24) and with the help of Eqs. (32) and (33), we obtain a system of nine non-homogeneous equations which can be written as:

$$\sum_{j=1}^{9} a_{ij} Z_j = Y_i\ ;\ \left(i = 1, 2, 3, 4, 5, 6, 7, 8, 9\right) \tag{34}$$

$$a_{1i} = -\left(d_1(1 - \frac{V_i^2}{V_0^2}\sin^2\theta_0) + d_2\frac{V_i^2}{V_0^2}\sin^2\theta_0\right)\frac{\omega^2}{V_i^2} - l_i + d_3 g_i, \quad a_{1j} = (d_2 - d_1)\frac{\omega^2}{V_j V_0}\sin\theta_0\sqrt{1 - \frac{V_j^2}{V_0^2}\sin^2\theta_0},$$

$$a_{18} = \left[\left(\bar{d}_1(1 - \frac{\bar{V}_1^2}{V_0^2}\sin^2\theta_0) + \bar{d}_2\frac{\bar{V}_1^2}{V_0^2}\sin^2\theta_0\right)\frac{\omega^2}{\bar{V}_1^2}\right], \quad a_{19} = (\bar{d}_2 - \bar{d}_1)\frac{\omega^2}{\bar{V}_2 V_0}\sin\theta_0\sqrt{1 - \frac{\bar{V}_2^2}{V_0^2}\sin^2\theta_0},$$

$$a_{2i} = -\left(2d_4 + d_5\right)\frac{\omega^2}{V_i V_0}\sin\theta_0\sqrt{1 - \frac{V_i^2}{V_0^2}\sin^2\theta_0},$$

$$a_{2j} = d_4\frac{\omega^2}{V_j^2}(1 - 2\frac{V_j^2}{V_0^2}\sin^2\theta_0) + d_5\frac{\omega^2}{V_j^2}(1 - \frac{V_j^2}{V_0^2}\sin^2\theta_0) - d_5 n_j,$$

$$a_{28} = -2\bar{d}_3\frac{\omega^2}{\bar{V}_1 V_0}\sin\theta_0\sqrt{1 - \frac{\bar{V}_1^2}{V_0^2}\sin^2\theta_0}, \quad a_{29} = -\left[\bar{d}_3\frac{\omega^2}{\bar{V}_2^2}\left(1 - 2\frac{\bar{V}_2^2}{V_0^2}\sin^2\theta_0\right)\right],$$

$$a_{3i} = \iota d_7 g_i\frac{\omega}{V_0}\sin\theta_0, \quad a_{3j} = \iota n_j\frac{\omega}{V_j}\sqrt{1 - \frac{V_j^2}{V_0^2}\sin^2\theta_0}, \quad a_{38} = a_{39} = 0,$$

$$a_{4i} = \iota d_8 \frac{\omega}{V_i}\sqrt{1-\frac{V_i^2}{V_0^2}\sin^2\theta_0}\; g_i\,, \quad a_{4j} = -\iota d_9 \frac{\omega}{V_0}\sin\theta_0 n_j\,, \quad a_{48} = a_{49} = 0,$$

$$a_{5i} = -\left(d_{10} + d_{11}\sqrt{1-\frac{V_i^2}{V_0^2}\sin^2\theta_0}\right)\frac{\omega^2}{V_i^2} f_i\,, \quad a_{5j} = -d_{11}\frac{\omega^2}{V_j V_0} m_j \sin\theta_0 \sqrt{1-\frac{V_j^2}{V_0^2}\sin^2\theta_0}\,, \quad a_{58} = a_{59} = 0\,,$$

$$a_{6i} = -\left(d_{12} + d_{13}\right) f_i \frac{\omega^2}{V_i V_0}\sin\theta_0 \sqrt{1-\frac{V_i^2}{V_0^2}\sin^2\theta_0}\,, \quad a_{6j} = (d_{13}(1-\frac{V_j^2}{V_0^2}\sin^2\theta_0) - d_{12}\frac{V_j^2}{V_0^2}\sin^2\theta_0) m_j \frac{\omega^2}{V_j^2}\,,$$

$$a_{68} = a_{69} = 0\,,$$

$$a_{7i} = \iota\frac{\omega}{V_0}\sin\theta_0\,, \quad a_{7j} = -\iota\frac{\omega}{V_j}\sqrt{1-\frac{V_j^2}{V_0^2}\sin^2\theta_0}\,, \quad a_{78} = -\iota\frac{\omega}{V_0}\sin\theta_0\,, \quad a_{79} = \iota\frac{\omega}{\overline{V}_2}\sqrt{1-\frac{\overline{V}_2^2}{V_0^2}\sin^2\theta_0}\,,$$

$$a_{8i} = \iota\frac{\omega}{V_i}\sqrt{1-\frac{V_i^2}{V_0^2}\sin^2\theta_0}\,, \quad a_{8j} = \iota\frac{\omega}{V_0}\sin\theta_0, \quad a_{88} = \iota\frac{\omega}{\overline{V}_1}\sqrt{1-\frac{\overline{V}_1^2}{V_0^2}\sin^2\theta_0}\,, \quad a_{89} = -\iota\frac{\omega}{V_0}\sin\theta_0\,,$$

$$a_{9i} = \iota l_i \frac{\omega}{V_i}\sqrt{1-\frac{V_i^2}{V_0^2}\sin^2\theta_0}\,, \quad a_{9j} = a_{98} = a_{99} = 0 \qquad (i = 1,\ 2,\ 3,\ 4 \text{ and } \quad j = 5,\ 6,\ 7) \tag{35}$$

where

$$d_1 = \frac{\rho c_1^2}{\nu T_0}, \quad d_2 = \frac{\lambda}{\nu T_0}, \quad d_3 = \frac{\lambda_0}{\nu T_0}, \quad d_4 = \frac{\mu}{\nu T_0}, \quad d_5 = \frac{K}{\nu T_0}, \quad d_6 = \frac{\gamma}{L^2 \nu T_0}, \quad d_7 = \frac{b_0}{L^2\nu T_0},$$

$$d_8 = \frac{\alpha_0}{L^2\nu T_0}, \quad d_9 = \frac{b_0}{L^2\nu T_0}, \quad d_{10} = \frac{k_4}{L^3 c_1 \nu T_0}, \quad d_{11} = \frac{k_5 + k_6}{L^3 c_1 \nu T_0}, \quad d_{12} = \frac{k_5}{L^3 c_1 \nu T_0}, \quad d_{13} = \frac{k_6}{L^3 c_1 \nu T_0},$$

$$\overline{d}_1 = \frac{\lambda^e + 2\mu^e}{\nu T_0}, \quad \overline{d}_2 = \frac{\lambda^e}{\nu T_0}, \quad \overline{d}_3 = \frac{\mu^e}{\nu T_0}$$

For incident LD-wave:

$$A^* = S_{01}\,, \; S_{02} = S_{03} = S_{04} = S_{05} = S_{06} = S_{07} = 0\,, \quad Y_1 = -a_{11}\,, \quad Y_2 = a_{21}\,, \quad Y_3 = -a_{31}\,, \quad Y_4 = a_{41}\,,$$
$$Y_5 = -a_{51}\,, \quad Y_6 = a_{61}\,, \quad Y_7 = -a_{71}\,, \quad Y_8 = a_{81}, \quad Y_9 = a_{91}$$

For incident T-wave:

$$A^* = S_{02}\,, \; S_{01} = S_{03} = S_{04} = S_{05} = S_{06} = S_{07} = 0, \; Y_1 = -a_{12}\,, \quad Y_2 = a_{22}\,, \quad Y_3 = -a_{32}, \quad Y_4 = a_{42}\,,$$
$$Y_5 = -a_{52}\,, \quad Y_6 = a_{62}\,, \quad Y_7 = -a_{72}\,, \; Y_8 = a_{82}, \quad Y_9 = a_{92}$$

For incident LM-wave:

$$A^* = S_{03}\,, \; S_{01} = S_{02} = S_{04} = T_{05} = T_{06} = T_{07} = 0\,, \quad Y_1 = -a_{13}\,, \quad Y_2 = a_{23}\,, \quad Y_3 = -a_{33}\,, \quad Y_4 = a_{43}\,,$$
$$Y_5 = -a_{53}\,, \quad Y_6 = a_{63}\,, \quad Y_7 = -a_{73}\,, \quad Y_8 = a_{83}, \quad Y_9 = a_{93}$$

For incident LT-wave:

$$A^* = S_{04}\,, \quad S_{01} = S_{02} = S_{03} = S_{05} = S_{06} = S_{07} = 0, \quad Y_1 = -a_{14}\,, \quad Y_2 = a_{24}\,, \quad Y_3 = -a_{34}\,, \quad Y_4 = a_{44}\,,$$
$$Y_5 = -a_{54}\,, \quad Y_6 = a_{64}\,, \quad Y_7 = -a_{74}\,, \quad Y_8 = a_{84}, \quad Y_9 = a_{94}$$

For incident CD-I wave:

$A^* = S_{05}$, $S_{01} = S_{02} = S_{03} = S_{04} = S_{06} = S_{07} = 0$, $Y_1 = a_{15}$, $Y_2 = -a_{25}$, $Y_3 = a_{35}$, $Y_4 = -a_{45}$,
$Y_5 = a_{55}$, $Y_6 = -a_{65}$, $Y_7 = a_{75}$, $Y_8 = -a_{85}$, $Y_9 = a_{95} = 0$

For incident CD-II wave:

$A^* = S_{06}$, $S_{01} = S_{02} = S_{03} = S_{04} = S_{05} = S_{07} = 0$, $Y_1 = -a_{14}$, $Y_2 = a_{24}$, $Y_3 = -a_{34}$, $Y_4 = a_{44}$,
$Y_5 = a_{56}$, $Y_6 = -a_{66}$, $Y_7 = a_{76}$, $Y_8 = -a_{86}$, $Y_9 = a_{96} = 0$

For incident CD-III wave:

$A^* = S_{06}$, $S_{01} = S_{02} = S_{03} = S_{04} = S_{05} = S_{06} = 0$, $Y_1 = -a_{14}$, $Y_2 = a_{24}$, $Y_3 = -a_{34}$, $Y_4 = a_{44}$,
$Y_5 = a_{57}$, $Y_6 = -a_{67}$, $Y_7 = a_{77}$, $Y_8 = -a_{87}$, $Y_9 = a_{97} = 0$

and

$$Z_1 = \frac{S_1}{A^*}, \quad Z_2 = \frac{S_2}{A^*}, \quad Z_3 = \frac{S_3}{A^*}, \quad Z_4 = \frac{S_4}{A^*}, \quad Z_5 = \frac{S_5}{A^*}, \quad Z_6 = \frac{S_6}{A^*}, \quad Z_7 = \frac{S_7}{A^*}, \quad Z_8 = \frac{\overline{S_1}}{A^*}, \quad Z_9 = \frac{\overline{T_1}}{A^*}$$

where $Z_1, Z_2, Z_3, Z_4, Z_5, Z_6, Z_7$ are the amplitude ratios of reflected LD-wave, T-wave, LM-wave, LT-wave and coupled CD-I, CD-II, CD-III waves in medium M_1 and Z_8, Z_9 are the amplitude ratios of transmitted P-wave and SV-wave in medium M_2.

5 PARTICULAR CASES

(a) If we neglect micropolarity effect in medium M_1 i.e $K = 0$, then we obtain amplitude ratios at an interface of microstretch thermoelastic half-space with microtemperatures without microtational effect and elastic solid half space as:

$$\sum_{j=1}^{8} a_{ij} Z_j = Y_i \; ; \; \left(i = 1, 2, 3, 4, 5, 6, 7, 8\right) \tag{36}$$

where the values of a_{ij} are given as:

$$a_{1i} = -\left(d_1 (1 - \frac{V_i^2}{V_0^2} \sin^2\theta_0) + d_2 \frac{V_i^2}{V_0^2} \sin^2\theta_0 \right) \frac{\omega^2}{V_i^2} - l_i + d_3 g_i \; , \quad a_{1j} = (d_2 - d_1) \frac{\omega^2}{V_j V_0} \sin\theta_0 \sqrt{1 - \frac{V_j^2}{V_0^2} \sin^2\theta_0} \; ,$$

$$a_{17} = \left[\left(\overline{d}_1 (1 - \frac{\overline{V_1^2}}{V_0^2} \sin^2\theta_0) + \overline{d}_2 \frac{\overline{V_1^2}}{V_0^2} \sin^2\theta_0 \right) \frac{\omega^2}{\overline{\overline{V_1^2}}} \right] \; , \quad a_{18} = (\overline{d}_2 - \overline{d}_1) \frac{\omega^2}{\overline{V}_2 V_0} \sin\theta_0 \sqrt{1 - \frac{\overline{V_2^2}}{V_0^2} \sin^2\theta_0} \; ,$$

$$a_{2i} = -\left(2 d_4 + d_5\right) \frac{\omega^2}{V_i V_0} \sin\theta_0 \sqrt{1 - \frac{V_i^2}{V_0^2} \sin^2\theta_0} \; , \quad a_{2j} = d_4 \frac{\omega^2}{V_j^2} (1 - 2\frac{V_j^2}{V_0^2} \sin^2\theta_0) + d_5 \frac{\omega^2}{V_j^2} (1 - \frac{V_j^2}{V_0^2} \sin^2\theta_0),$$

$$a_{27} = -2\overline{d}_3 \frac{\omega^2}{\overline{\overline{V}_1} V_0} \sin\theta_0 \sqrt{1 - \frac{\overline{V_1^2}}{V_0^2} \sin^2\theta_0} \; , \quad a_{28} = -\left[\overline{d}_3 \frac{\omega^2}{\overline{\overline{V_2^2}}} \left(1 - 2\frac{\overline{V_2^2}}{V_0^2} \sin^2\theta_0 \right) \right],$$

$$a_{3i} = \iota d_8 \frac{\omega}{V_i} \sqrt{1 - \frac{V_i^2}{V_0^2} \sin^2\theta_0} \; g_i \; , \quad a_{3j} = -\iota d_9 \frac{\omega}{V_0} \sin\theta_0 n_j \; , \quad a_{37} = a_{38} = 0,$$

$$a_{4i}=-\left(d_{10}+d_{11}\sqrt{1-\frac{V_i^2}{V_0^2}\sin^2\theta_0}\right)\frac{\omega^2}{V_i^2}f_i\ ,\quad a_{4j}=-d_{11}\frac{\omega^2}{V_jV_0}m_j\sin\theta_0\sqrt{1-\frac{V_j^2}{V_0^2}\sin^2\theta_0}\ ,$$

$$a_{47}=a_{48}=0\ ,\quad a_{5i}=-\left(d_{12}+d_{13}\right)f_i\frac{\omega^2}{V_iV_0}\sin\theta_0\sqrt{1-\frac{V_i^2}{V_0^2}\sin^2\theta_0}\ , \tag{37}$$

$$a_{5j}=(d_{13}(1-\frac{V_j^2}{V_0^2}\sin^2\theta_0)-d_{12}\frac{V_j^2}{V_0^2}\sin^2\theta_0)\frac{\omega^2}{V_j^2}\ ,\quad a_{57}=a_{58}=0\ ,\ ,$$

$$a_{6i}=\iota\frac{\omega}{V_0}\sin\theta_0\ ,\quad a_{6j}=-\iota\frac{\omega}{V_j}\sqrt{1-\frac{V_j^2}{V_0^2}\sin^2\theta_0}\ ,a_{67}=-\iota\frac{\omega}{V_0}\sin\theta_0\ ,\quad a_{68}=\iota\frac{\omega}{\overline{V}_2}\sqrt{1-\frac{\overline{V}_2^2}{V_0^2}\sin^2\theta_0}\ ,$$

$$a_{7i}=\iota\frac{\omega}{V_i}\sqrt{1-\frac{V_i^2}{V_0^2}\sin^2\theta_0}\ ,\quad a_{7j}=\iota\frac{\omega}{V_0}\sin\theta_0\ ,\quad a_{77}=\iota\frac{\omega}{\overline{V}_1}\sqrt{1-\frac{\overline{V}_1^2}{V_0^2}\sin^2\theta_0}\ ,$$

$$a_{78}=-\iota\frac{\omega}{V_0}\sin\theta_0\ ,\quad a_{8i}=\iota l_i\frac{\omega}{V_i}\sqrt{1-\frac{V_i^2}{V_0^2}\sin^2\theta_0}\ ,\quad a_{8j}=a_{87}=a_{88}=0$$

$(i=1,\ 2,\ 3,\ 4$ and $\quad j=5,\ 6)$

6 NUMERICAL RESULTS AND DISCUSSION

The following values of relevant parameters are taken for numerical computations. Following Eringen [32], the values of micropolar constants are taken as:

$$\lambda=9.4\times10^{10}Nm^{-2}\ ,\ \mu=4.0\times10^{10}Nm^{-2}\ ,\ K=1.0\times10^{10}Nm^{-2}\ ,\quad \gamma=7.779\times10^{-8}N\ ,$$
$$j=2\times10^{-20}m^2\ ,\quad \rho=1.74\times10^3Kgm^{-3}\ .$$

and thermal parameters are taken from Dhaliwal and Singh [33]:

$$c^*=1.04\times10^3NmKg^{-1}K^{-1}\ ,\quad T_0=0.298K\ ,\quad K^*=1.7\times10^2Nsec^{-1}K^{-1}\ .$$

Microstretch parameters are taken as:

$$j_0=0.19\times10^{-17}m^2,\quad b=0.15\times10^{-9}N\ ,\quad \lambda_0=0.21\times10^{11}Nm^{-2},\quad \lambda_1=0.007\times10^{12}Nm^{-2},$$
$$\alpha_0=0.00008\times10^{-5}N$$

and microtemperatures parameters are taken as:

$$k_1=0.0035Ns^{-1},\quad k_2=0.045Ns^{-1},\ k_3=0.055NK^{-1}s^{-1},\ k_4=0.065Ns^{-1}m^2,\ k_5=0.076Ns^{-1}m^2,$$
$$k_6=0.096Ns^{-1}m^2,\ \mu_1=0.0085N\ ,\quad \mu_2=0.0095N$$

The values of amplitude ratios have been computed at different angles of incidence. In Figs.1-18, MMT corresponds to microstretch thermoelastic solid with microtemperatures and WMP corresponds to microstretch thermoelastic solid with microtemperatures without microrotational effect.

6.1 Incident LD-Wave

Variations of amplitude ratios $|Z_i|;1 \le i \le 9$ with the angle of incidence θ_0, for incident LD-wave are shown in Figs. 2 through 10. Fig. 2 shows that the values of $|Z_1|$ for MMT decrease monotonically in the range $0^0 < \theta_0 < 77^0$ and then increase, where as the values for WMP increase monotonically in the range $0^0 < \theta_0 < 64^0$ and then decrease in the further range. It is noticed that the values for WMP are greater than the values for MMT in the whole range.

It is evident from Fig. 3 that the values of amplitude ratio $|Z_2|$ for MMT first increase and then decrease near the grazing incidence. The values for WMP follow oscillatory pattern in the whole range. The values for WMP in comparison in comparision with MMT are greater in the whole range, except near the normal incidence and grazing incidence. Fig. 4 shows that the values for $|Z_3|$ for MMT decrease in the whole range. The values for WMP attain maximum value in the intermediate range. The values for MMT are greater than the values for WMP in the whole range, except the range $39^0 < \theta_0 < 76^0$, where the behavior is reversed. Fig. 5 depicts that the values of amplitude ratio $|Z_4|$ for MMT decrease from normal incidence to grazing incidence. The values for WMP are greater than the values for MMT in the range $20^0 < \theta_0 < 80^0$. The values of amplitude ratio for MMT and WMP are magnified by multiplying by 10^6.

Fig. 6 shows that the values of $|Z_5|$ for WMP attain maximu value at the normal incidence. The values of amplitude ratio for MMT and WMP are magnified by multiplying by10. The values for MMT increase in the range $0^0 < \theta_0 < 61^0$ and then decrease. Fig. 7 shows that the values of $|Z_6|$ for MMT increase monotonically in the interval $0^0 < \theta_0 < 61^0$ and the decrease as θ_0 increases further, while the values for WMP decrease monotonically in the whole range. It is noticed from Fig. 8 that the values of $|Z_7|$ for MMT increase to attain maximum value at $\theta_0 = 55^0$ and then decrease with further increase in θ_0. The values for MMT are magnified by multiplying by 10^2. It is noticed from Fig. 9 that values of $|Z_8|$ for MMT decrease with increase in θ_0. The values for WMP oscillate and attain maximum value at normal incidence. Fig. 10 depicts that the values of amplitude ratio $|Z_9|$ for MMT increase in the interval $0^0 < \theta_0 < 65^0$ and decrease for $\theta_0 \ge 65^0$. The values for MMT are greater in comparison to the values for WMP in the whole range. The values of amplitude ratio for WMP are magnified by multiplying by 10^2.

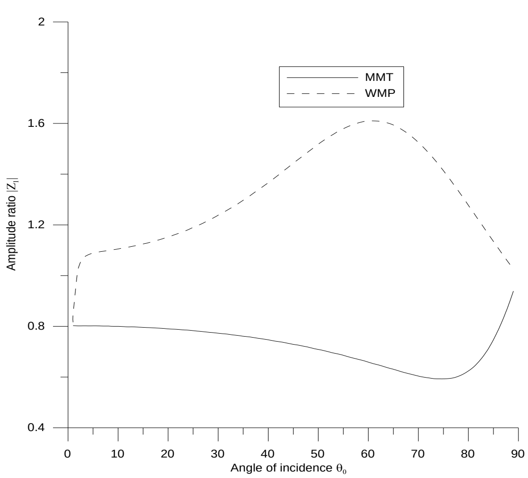

Fig. 2
Variations of amplitude ratios $|Z_1|$ with the angle of incidence for LD-Wave.

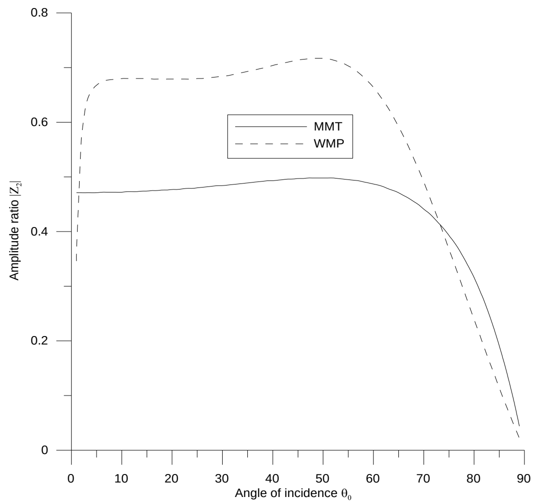

Fig. 3
Variations of amplitude ratios $|Z_2|$ with the angle of incidence for LD-Wave.

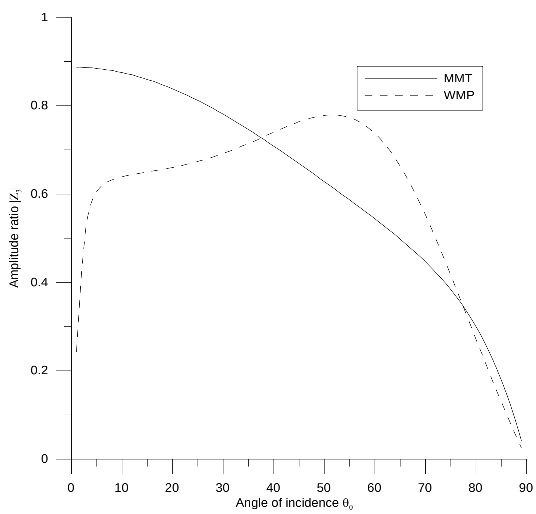

Fig. 4
Variations of amplitude ratios $|Z_3|$ with the angle of incidence for LD-Wave.

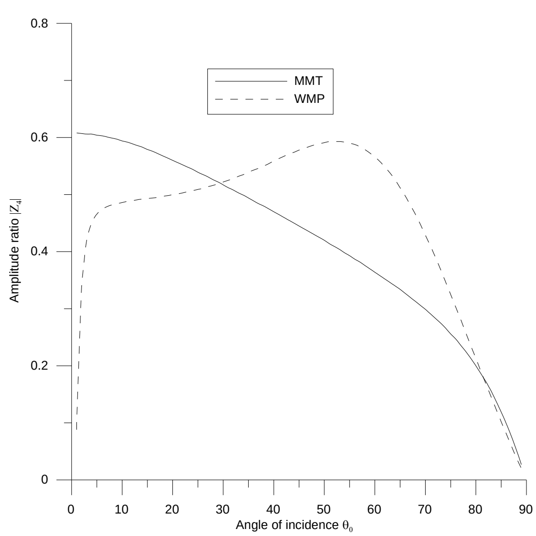

Fig. 5
Variations of amplitude ratios $|Z_4|$ with the angle of incidence for LD-Wave.

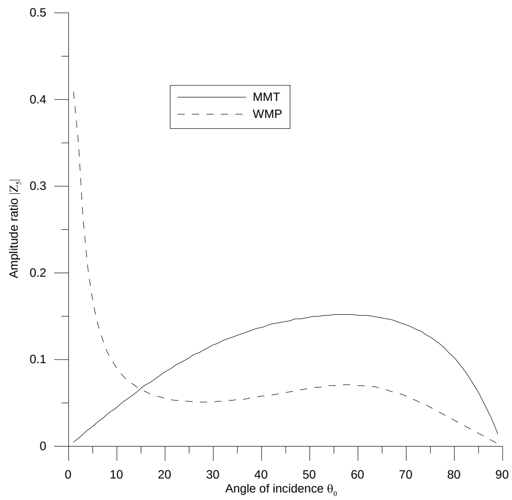

Fig. 6
Variations of amplitude ratios $|Z_5|$ with the angle of incidence for LD-Wave.

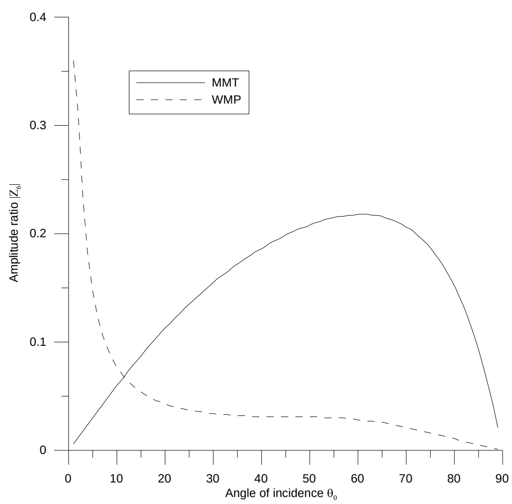

Fig. 7
Variations of amplitude ratios $|Z_6|$ with the angle of incidence for LD-Wave.

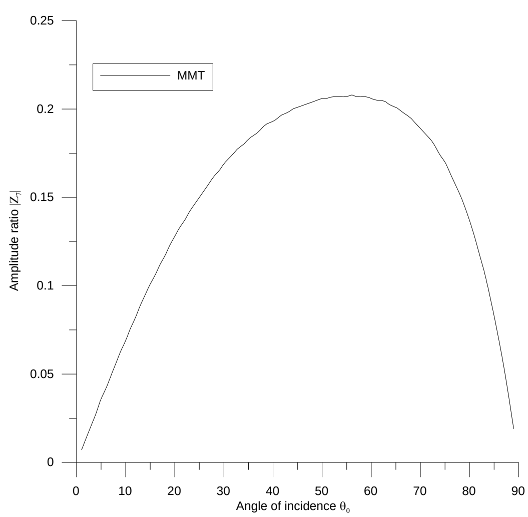

Fig. 8
Variations of amplitude ratios $|Z_7|$ with the angle of incidence for LD-Wave.

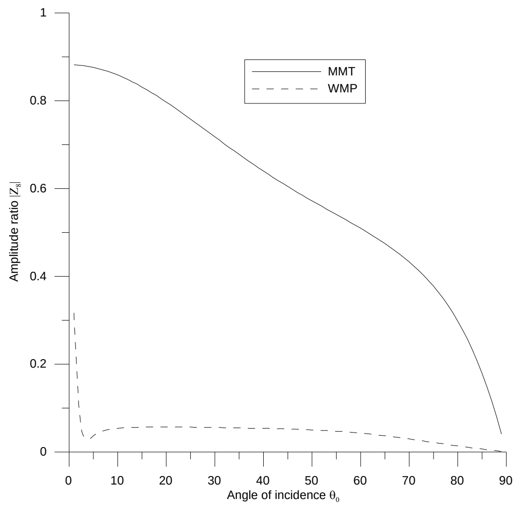

Fig. 9
Variations of amplitude ratios $|Z_8|$ with the angle of incidence for LD-Wave.

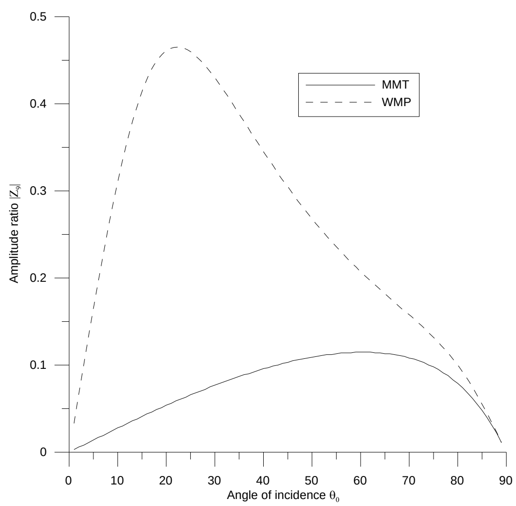

Fig. 10
Variations of amplitude ratios $|Z_9|$ with the angle of incidence for LD-Wave.

6.2 Incident LM-Wave

Variations of amplitude ratios $|Z_i|; 1 \le i \le 9,$ with the angle of incidence θ_0, for incident LM-wave are shown in Figs. 11 through 19. Figs. 11 show that the values of $|Z_1|$ for MMT decrease and WMP oscillate in the whole range. The values for WMP remain more than the values for MMT in the whole range. Fig. 12 depicts that the values of $|Z_2|$ for WMP are greater than the values for MMT in the whole range. It is evident from Fig. 13 that the values of $|Z_3|$ for WMP attain maximum value in the range $65^0 < \theta_0 < 75^0$. The values for WMP in comparison to the values for MMT are more in the whole range.

Fig. 14 depicts that values of $|Z_4|$ for MMT oscillate and attain maximum value near the normal incidence. The values of amplitude ratio for MMT are magnified by multiplying by 10^6 and WMP are magnified by multiplying by 10^5. Fig. 15 shows that the values of $|Z_5|$ for MMT increase in the range $0^0 < \theta_0 < 45^0$ and then decrease in further range. The values for WMP follow oscillatory pattern and attain peak value at $\theta_0 = 0^0$. The values of amplitude ratio for MMT and WMP are magnified by multiplying by 10. Fig. 16 shows that the values of $|Z_6|$ for MMT increase in the interval $0^0 < \theta_0 < 55^0$ and then decrease in the subsequent range, while the values for WMP decrease sharply in the whole range with slight oscillation in the finite region. Fig. 17 shows that the values of $|Z_7|$ for MMT get increased to attain maximum value in the intermediate range and then decrease sharply in the further range. The values of amplitude ratio for WMP are magnified by multiplying by 10^2. Fig. 18 shows that the values of $|Z_8|$ for MMT decrease and WMP oscillate in the whole range and the values for MMT remain more as compared to the values for WMP in the whole range, except near the normal incidence where the behavior is reversed. Fig. 19 depicts that the values of amplitude ratio for MMT increase in the range $0^0 < \theta_0 < 56^0$ and then get decreased with increase in θ_0. The values of amplitude ratio for WMP attain peak values in the range $65^0 < \theta_0 < 75^0$. The values of amplitude ratio for MMT and WMP are magnified by multiplying by 10.

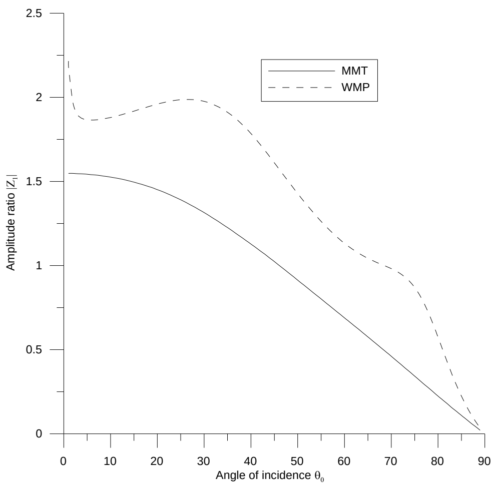

Fig. 11
Variations of amplitude ratios $|Z_1|$ with the angle of incidence for T-Wave.

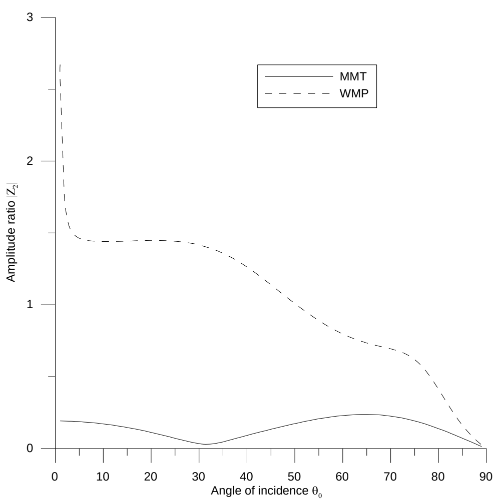

Fig. 12
Variations of amplitude ratios $|Z_2|$ with the angle of incidence for T-Wave.

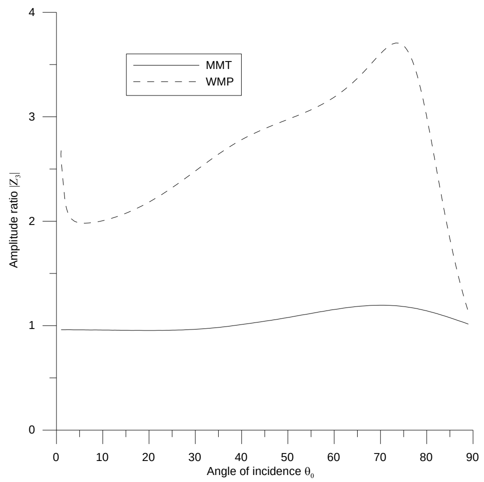

Fig. 13
Variations of amplitude ratios $|Z_3|$ with the angle of incidence for T-Wave.

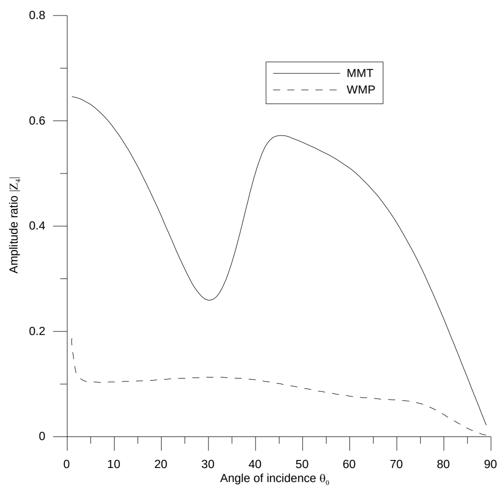

Fig. 14
Variations of amplitude ratios $|Z_4|$ with the angle of incidence for T-Wave.

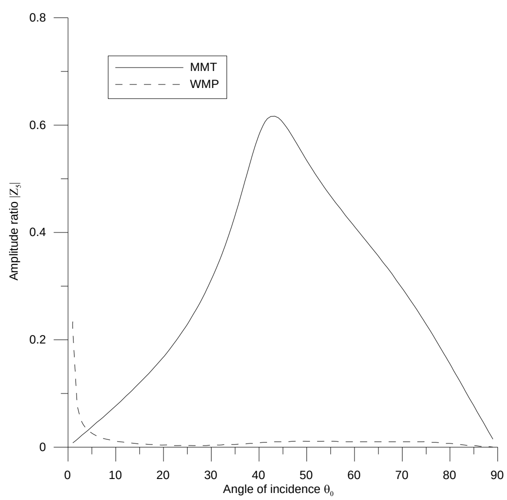

Fig. 15
Variations of amplitude ratios $|Z_5|$ with the angle of incidence for T-Wave.

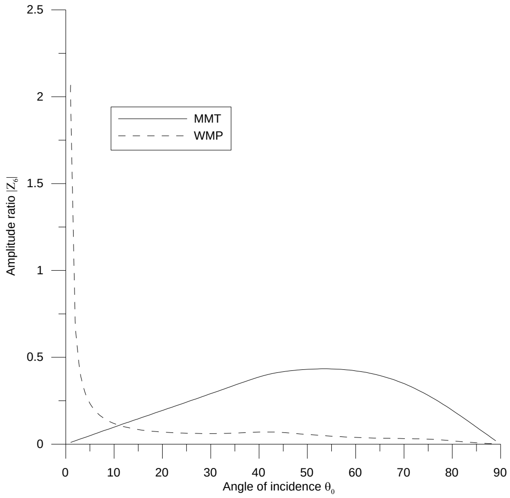

Fig.16
Variations of amplitude ratios $|Z_6|$ with the angle of incidence for T-Wave.

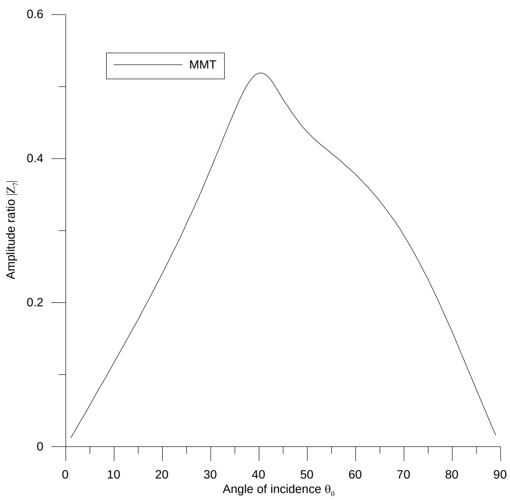

Fig.17
Variations of amplitude ratios $|Z_7|$ with the angle of incidence for T-Wave.

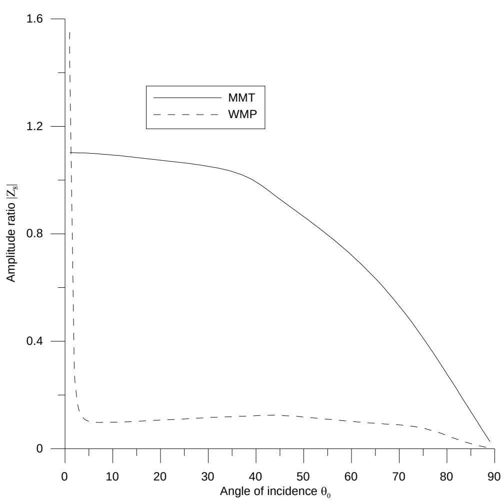

Fig.18
Variations of amplitude ratios $|Z_8|$ with the angle of incidence for T-Wave.

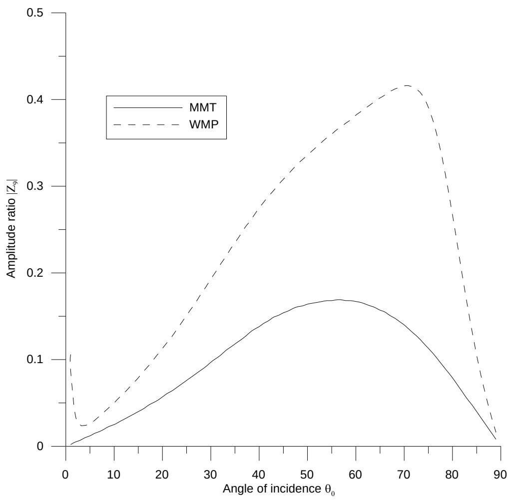

Fig.19
Variations of amplitude ratios $|Z_9|$ with the angle of incidence for T-Wave.

7 CONCLUSIONS

The reflection and transmission coefficients at an interface of microstretch thermoelastic solid half-space with microtemperatures and elastic solid half-space have been studied in the present paper. The amplitude ratios for an incidence of LD-wave and LM-wave have been obtained numerically and their variations with angle of incidence have been shown graphically. It is noticed that when LM-wave is incident, the values of reflected LD-wave, T-wave, LM-wave, LT-wave, transmitted SV-wave and when LD-wave is incident, the values of reflected LD-wave and transmitted SV-wave for WMP (without microrotational effect) are greater as compared to the values for MMT (with microrotational effect). The amplitude ratios for WMP are more oscillatory and attain peak value in the initial range.

REFERENCES

[1] Eringen A.C., 1966, Mechanics of micromorphic materials, *Proceedings of the 2nd International Congress of Applied Mechanics*, Springer, Berlin, 131-138.
[2] Eringen A.C., 1968, *Mechanics of Micromorphic Continua*, Mechanics of Generalized Continua, IUTAM Symposium, Freudenstadt-Stuttgart, Springer, Berlin, 18-35.
[3] Eringen A.C., 1971, *Micropolar Elastic Solids with Stretch***,** Ari Kitabevi Matbassi **24**:1-18.
[4] Eringen A.C., 1990, Theory of thermo-microstretch elastic solids, *International Journal of Engineering Science* **28**: 1291-1301.
[5] Grot R.A., 1969, Thermodynamics of a continuum with microstructure, *International Journal of Engineering Science* **7**: 801–814.
[6] Riha P., 1976, On the microcontinuum model of heat conduction in materials with inner structure, *International Journal of Engineering Science* **14**: 529-535.
[7] Iesan D., Quintanilla R., 2000, On a theory of thermoelasticity with microtemperatures, *Journal of Thermal Stresses* **23**:199–215.
[8] Ciarletta M., Scalia A., 2004, Some results in linear theory of thermomicrostretch elastic solids, *Meccanica* **39**:191-206.
[9] Iesan D., Quintanilla R., 2005, Thermal stresses in microstretch elastic plates, *International Journal of Engineering Science* **43**: 885-907.
[10] Othman M.I.A, Lofty K.H., Farouk R.M., 2010, Generalized thermo-microstretch elastic medium with temperature dependent properties for different theories, *Engineering Analysis with Boundary Elements* **43** :229-237.
[11] Passarella F., Tibullo V., 2010, Some results in linear theory of thermoelasticity backward in time for microstretch materials, *Journal of Thermal Stresses* **33**:559-576.
[12] Marin M., 2010, A partition of energy in thermoelasticity of microstretch bodies, *Nonlinear Analysis-Real World Applications* **11**(4): 2436-2447.

[13] Marin M., 2010, Lagrange identity method for microstretch thermoelastic materials, *Journal of Mathematical Analysis and Applications* **363**:275-286.
[14] Kumar S., Sharma J.N., Sharma Y.D., 2011, Generalized thermoelastic waves in microstretch plates loaded with fluid of varying temperature, *International Journal of Applied Mechanics* **3**:563-586.
[15] Othman M.I.A., Lofty K.H., 2010, On the plane waves of generalized thermomicrostretch elastic half space under three theories, *International Communications in Heat and Mass Transfer* **37**:192-200.
[16] Othman M.I.A., Lofty K.H., 2011, Effect of rotation on plane waves in generalized thermo-microstretch elastic solid with one relaxation time, *Multidiscipline Modelling in Materials and Structures* **7**:43-62.
[17] Kumar R., Rupender, 2008, Reflection at free surface of magneto-thermo-microstretch elastic solid, *Bulletin of Polish Academy of Sciences* **56**:263-271.
[18] Kumar R., Rupender, 2012, Propagation of plane waves at imperfect boundary of elastic and elctro-microstretch generalized thermoelastic solids, *Applied Mathematics and Mechanics* **30**:1445-1454.
[19] Shaw S., Mukhopadhayay B., 2012, Electromagnetic effects on rayleigh surface wave propagation in a homogeneous isotropic thermo-microstretch elastic half-space, *Journal of Engineering Physics and Thermophysics* **85** :229-238.
[20] Iesan D., 2001, On a theory of micromorphic elastic solids with microtemperatures, *Journal of Thermal Stresses* **24**: 737-752.
[21] Iesan D., Quintanilla R., 2009, On thermoelastic bodies with inner structure and microtemperatures, *Journal of Mathematical Analysis and Applications* **354**:12-23.
[22] Casas P.S., Quintanilla R., 2005, Exponential stability in thermoelasticity with microtemperatures, *International Journal of Engineering Science* **43**:33-47.
[23] Scalia A., Svanadze M., 2006, On the representation of solutions of the theory of thermoelasticity with microtemperatures, *Journal of Thermal Stresses* **29**: 849-863.
[24] Iesan D., 2006, Thermoelasticity of bodies with microstructure and microtemperatures, *International Journal of Solids and Structures* **43**: 3414-3427.
[25] Aouadi M., 2008, Some theorems in the isotropic theory of microstretch thermoelasticity with microtemperatures, *Journal of Thermal Stresses* **31**:649-662.
[26] Scalia A., Svanadze M., Tracinà R., 2010, Basic theorems in the equilibrium theory of thermoelasticity with microtemperatures peratures, *Journal of Thermal Stresses* **33**:721-753.
[27] Quintanilla R., 2011, On growth and continous dependence in thermoelasticity with microtemperatures, *Journal of Thermal Stresses* **34**:911-922.
[28] Steeb H., Singh J., Tomar S.K., 2013, Time harmonic waves in thermoelastic material with microtemperatures, *Mechanics Research Communications* **48**:8-18.
[29] Chirita S., Ciarletta M., Apice C.D., 2013, On the theory of thermoelasticity with microtemperatures, *Journal of Mathematical Analysis and Applications* **397**:349-361.
[30] Iesan D., 2007, Thermoelasticity of bodies with microstructure and microtemperatures, *International Journal of Solids and Structures* **44**:8648-8662.
[31] Bullen K.E., 1963, *An Introduction of the Theory of Seismology*, Cambridge University Press, Cambridge.
[32] Eringen A.C., 1984, Plane waves in non local micropolar elasticity, *International Journal of Engineering Science* **22**: 1113-1121.
[33] Dhaliwal R.S., Singh A.,1980, *Dynamic Coupled Thermoelasticity*, Hindustan Publication Corporation, New Delhi, India .